



# POSTBUCKLING BEHAVIOUR OF ISOTROPIC THIN RECTANGULAR PLATES WITH ONE FREE EDGE

ADAH E. I., ONWUKA D. O., IBEARUGBULEM O. M., UBI S. E., Nwigwe E. E.

(Received 14 September 2021; Revision Accepted 5 October 2021)

## ABSTRACT

This work aims to evaluate the individual stiffness of six plates' boundary conditions with one free edge to obtain the specific mathematical models for predicting the postbuckling loads of the six plates' boundary conditions under consideration. The shape profiles of each of the six plates were differentiated and substituted into the individual stiffness integrals to obtain the numerical values of the individual stiffness. The individual stiffness values were then substituted into the total bending and membrane stiffness expressions and evaluated. The resulting total and membrane stiffness expressions were thereafter substituted into the general postbuckling equation and evaluated to obtain specific mathematical models for the six plate types to predict the postbuckling loads of each plate. The newly formulated mathematical models were validated by carrying out numerical predictions of the postbuckling loads of each plate. The critical load obtained was compared with those in the literature and was found adequate. Additionally, the results showed a gradual increase in the strength of plate beyond the initial yield point which is in line with the behavior of plates. Based on these observations it was concluded that the newly formulated mathematical models for predicting the postbuckling strength of thin isotropic rectangular plates considered here were adequate and that the models will provide an easy means of analyzing thin plates for postbuckling loads.

**KEYWORDS:** Postbuckling Load, Mathematical Models, Polynomial Shape Functions, Rectangular Plates, Free Edge, Boundary Conditions

## INTRODUCTION

Unlike columns, plates possess additional strength beyond their initial yield points. The importance of plates in structural engineering practice such as aerospace and shipbuilding industries has over the years generated interest by many scholars to investigate the behavior of plates beyond the initial yield point. This is to harness the lightweight benefits of these types of structures. Earlier

Scholars who worked on this subject were Byklum and Amdahl (2002), Tanriöver and Senocak (2004), Elsheikh & Wang (2005), GhannadPour and Alinia (2006), Shufrin, Rabinovitch, and Eisenberger, (2008). Yoo and Lee (2011) examined the stress pattern for a square plate simply supported on all four edges and subjected to a uniform compressive force,  $N_x$ , in the postbuckling range. They used the assumed double trigonometric functions as deflected shape functions  $w$ . Paik, et. al. (2012) analyzed the elastic

**Adah E. I.**, Department of Civil and Environmental Engineering, University of Calabar, Nigeria.

**Onwuka D. O.**, Department of Civil Engineering, Federal University of Technology Owerri, Nigeria

**Ibearugbulem O. M.**, Department of Civil Engineering, Federal University of Technology Owerri, Nigeria

**Ubi S. E.**, Department of Civil Engineering, University of Cross River State, Calabar, Nigeria

**Nwigwe E. E.** Department of Civil and Environmental Engineering, University of Calabar, Nigeria.

large deflection behavior for metal plates under nonuniformly distributed lateral pressure with in-plane loads. They solved the modified Von Karman's fundamental nonlinear equations by assuming deflected function,  $w$ . Muradova and Stavroulakis (2012) investigated the postbuckling behavior of a rectangular Von Karman plate unilaterally resting on a nonlinear elastic foundation using the spectral method. Ibearugbulem et al. (2013), presented a technique for the inelastic buckling analysis of a thin rectangular isotropic plate under uniform in-plane compression in the longitudinal direction. They used Taylor's series to approximate the displacement function for a CCCC plate to solve Stowell's material nonlinearity

governing differential equations. Eziefula et al. (2014) solved for the plastic buckling analysis of a CSSS thin rectangular isotropic plate under uniform in-plane compression in the longitudinal direction. Oghuaghambba (2015) undertook a closed-form analysis of buckling and postbuckling loads of isotropic thin rectangular plates of various support conditions. He used Euler direct integration method to solve von Karman's large deflection equation and obtain the general postbuckling equation as Equation (1). He applied "work principle and minimum work error theory" to evaluate the buckling and postbuckling loads, as well as the critical loads.

He obtained the following general postbuckling equation,  $N_x$ .

$$N_x = \frac{\frac{49}{484} \int_0^1 \int_0^1 \left( \frac{\partial^4 h_1}{p^2 \partial R^4} \cdot h_1 + 2 \frac{\partial^2 h_1}{\partial R^2 \partial Q^2} \cdot h_1 + p^2 \frac{\partial^4 h_1}{\partial Q^4} \cdot h_1 \right) \cdot h_1 dR dQ}{\int_0^1 \int_0^1 \left( \frac{\partial^2 h_1}{\partial R^2} \cdot h_1 \right) dR} \frac{D\pi^2}{b^2} + \frac{\frac{294}{121} (1-\nu^2) p^2 W_{uv}^2 \int_0^1 \int_0^1 \left( \frac{\partial^2 h_1 \partial^2 h_2}{\partial Q^2 \partial R^2} + \frac{\partial^2 h_1 \partial^2 h_2}{\partial R^2 \partial Q^2} - 2 \frac{\partial^2 h_1 \partial^2 h_2}{\partial R \partial Q \partial R \partial Q} \right) \cdot h_1 dR dQ}{(1+2p^2+p^4)t^2 \int_0^1 \int_0^1 \left( \frac{\partial^2 h_1}{\partial R^2} \cdot h_1 \right) dR} \frac{D\pi^2}{b^2} \quad (1)$$

where,  $W_{uv}^2$  is stress function coefficient for a plate under post-buckling regime,  $p$  is aspect ratio,  $\frac{a}{b}$ ,  $t$  is plate thickness,  $h_1$  is non-coefficient stress function of a slightly bent plate,  $h_2$  is non-coefficient stress function of a slightly bent plate. Elsami (2018) stated that postbuckling behavior of rectangular plate hinges mostly on von-Karman type nonlinear strain-displacement relations which is given here in as

$$\varepsilon_{xx} = -z \frac{\partial^2 w}{\partial x^2} + \left[ \frac{1}{2} \left( \frac{\partial w}{\partial x} \right)^2 + \frac{\partial u_0}{\partial x} \right] \quad (2)$$

$$\varepsilon_{yy} = -z \frac{\partial^2 w}{\partial y^2} + \left[ \frac{1}{2} \left( \frac{\partial w}{\partial y} \right)^2 + \frac{\partial v_0}{\partial y} \right] \quad (3)$$

Where the first term is the bending term and the second term is the membrane term.  $u_0$  and  $v_0$  are the middle surface deformations that are no longer zero as assumed in small deformation theory. Enem (2018) and Onodagu (2018) also worked on pure bending and free vibration of plates under large deformation using energy principles. Adah (2019), modified Iyengar's equation by determining the numerical factor for modulus of rigidity in the inelastic range. He proposed two different equations for the post-buckling loads and stresses of the SSSS rectangular plate. Ibearugbulem et al. (2020) formulated a general mathematical model for buckling and postbuckling analysis of isotropic thin plates. This they did based on the equation (2) and (3). They applied this general equation to a plate simply supported all round based on trigonometric shape profile. Just like many other scholars, much effort has been expended on this simple case. None of the researchers has subjected this equation to thorough scrutiny with other boundary conditions especially those with one free edge to ascertain the suitability of this equation.

Therefore, the present work based on the use of a polynomial shape profile is aimed at evaluating six plate boundary conditions with one free edge to obtain individual stiffness. And based on these stiffnesses the total bending and membrane stiffness will be formulated. Afterward, these will be substituted into the general postbuckling equation to formulate the specific postbuckling models to predict the postbuckling load of the six plates considered here.

**METHODOLOGY**

**The General Postbuckling Governing Equation**

Ibearugbulem et al. (2020) derived a general mathematical model for buckling and postbuckling analysis of isotropic thin plates as Equation (4)

$$N_x = \left[ \frac{k_{bT}}{k_{Nx}} + \frac{3 k_{mT}}{2 k_{Nx}} \frac{1}{(h_{max})^2} \left( \frac{w}{t} \right)^2 \right] \frac{D}{a^2} \quad (4)$$

Where the total bending stiffness,  $K_{bT}$ , and membrane stiffness,  $K_{mT}$ , are expressed as

$$K_{bT} = \left[ k_{bx} + \frac{2k_{bxy}}{2^2} + \frac{k_{by}}{2^4} \right] \quad (5)$$

$$K_{mT} = \left[ k_{mx} + \frac{2k_{mxy}}{2^2} + \frac{k_{my}}{2^4} \right] \quad (6)$$

And the individual stiffnesses are expressed as

$$k_{bx} = \int_0^1 \int_0^1 \left( \frac{\partial^2 h}{\partial R^2} \right)^2 dRdQ \quad (7)$$

$$k_{bxy} = \int_0^1 \int_0^1 \left( \frac{\partial^2 h}{\partial R \partial Q} \right)^2 dRdQ \quad (8)$$

$$k_{by} = \int_0^1 \int_0^1 \left( \frac{\partial^2 h}{\partial Q^2} \right)^2 dRdQ \quad (9)$$

$$k_{mx} = \int_0^1 \int_0^1 \left( \frac{\partial h}{\partial R} \right)^4 dRdQ \quad (10)$$

$$k_{mxy} = \int_0^1 \int_0^1 \left( \frac{\partial h}{\partial R} \right)^2 \left( \frac{\partial h}{\partial Q} \right)^2 dRdQ \quad (11)$$

$$k_{my} = \int_0^1 \int_0^1 \left( \frac{\partial h}{\partial Q} \right)^4 dRdQ \quad (12)$$

$$k_{Nx} = \int_0^1 \int_0^1 \left( \frac{\partial h}{\partial R} \right)^2 dRdQ \quad (13)$$

Subscript b and m denote the bending and membrane. W is the deflected shape function, h is the shape profile, a is the plate dimension along the x-axis, and D is the flexural rigidity of the plate given as

$$D = \frac{Et^3}{12(1-\nu^2)} \quad (14)$$

Equation (4) can be rewritten as

$$N_x = \frac{k_{bT}}{k_{Nx}} \frac{D}{a^2} + \frac{3 k_{mT}}{2 k_{Nx}} \frac{1}{(h_{max})^2} \left( \frac{w}{t} \right)^2 \frac{D}{a^2} \quad (15)$$

The first term at the right-hand side is the critical load of the plate while the second term is the additional load that the plate can carry beyond the initial yield point before failure occurs (that is postbuckling term).

**Polynomial Deflected Shape Functions**

The primary aim of this work as stated earlier is to evaluate the individual stiffness based on the individual plate deflection shape functions of each plate boundary condition, to obtain the total bending and membrane stiffness. These will thereafter be substituted into the general postbuckling equation to obtain the specific mathematical models for the six plate boundary conditions under consideration. Therefore, the polynomial deflected shape functions of the six plates considered here are presented in Table 1 as given by Ibearugbulem et al. (2014).

Table 1: Plate Type and Shape Parameter for Six Boundry Conditions

PLATE TYPES	SHAPE PROFILE (h) W = Ah; (i.e h = R strip x Q strip)
SSFS	$(R - 2Q^3 + Q^4) \left( \frac{7}{3}Q - \frac{10}{3}Q^3 + \frac{10}{3}Q^4 - Q^5 \right)$
SCFS	$(1.5R^2 - 2R^3 + R^4) \left( \frac{7}{3}Q - \frac{10}{3}Q^3 + \frac{10}{3}Q^4 - Q^5 \right)$
CSFS	$(R - 2R^3 + R^4)(2.8Q^2 - 5.2Q^3 + 3.8Q^4 - Q^5)$
CCFS	$(1.5R^2 - 2R^3 + R^4)(2.8Q^2 - 5.2Q^3 + 3.8Q^4 - Q^5)$
SCFC	$(R^2 - 2R^3 + R^4) \left( \frac{7}{3}Q - \frac{10}{3}Q^3 + \frac{10}{3}Q^4 - Q^5 \right)$
CCFC	$(R^2 - 2R^3 + R^4)(2.8Q^2 - 5.2Q^3 + 3.8Q^4 - Q^5)$

Note: S means simply supported edge, C means Clamped Edged, and F means Free Edge

### Evaluation of stiffness

**Evaluation of SSFS plate stiffnesses at the point of Maximum Deflection (R = 0.5, Q = 1) are as follows:**

From Table 1, the polynomial deflected shape function for SSFS plate is given as

$$h = (R - 2Q^3 + Q^4) \left( \frac{7}{3}Q - \frac{10}{3}Q^3 + \frac{10}{3}Q^4 - Q^5 \right) \quad (16)$$

$$h_x = (R - 2Q^3 + Q^4) \quad (17)$$

$$h_y = \left( \frac{7}{3}Q - \frac{10}{3}Q^3 + \frac{10}{3}Q^4 - Q^5 \right) \quad (18)$$

Therefore, differentiating the shape profile for SSFS plate and substituting into the Equations (7-13) and carrying out the evaluation as follows:

$$\begin{aligned}
 k_{bx} &= \int_0^1 \int_0^1 \left( \frac{\partial^2 h}{\partial R^2} \right)^2 dR dQ = \int_0^1 \left( \frac{\partial^2 h_x}{\partial R^2} \right)^2 \partial R * \int_0^1 h_y^2 \partial Q \\
 k_{bx} &= \int_0^1 (-12R + 12R^2)^2 \partial R * \int_0^1 \left( \frac{7}{3}Q - \frac{10}{3}Q^3 + \frac{10}{3}Q^4 - Q^5 \right)^2 \partial Q \\
 k_{bx} &= \int_0^1 (144R^2 - 288R^3 + 144R^4) \partial R * \int_0^1 \left( \frac{49}{9}Q^2 - \frac{140}{9}Q^4 + \frac{140}{9}Q^5 + \frac{58}{9}Q^6 - \frac{200}{9}Q^7 + \frac{160}{9}Q^8 \right. \\
 &\quad \left. - \frac{20}{3}Q^9 + Q^{10} \right) \partial Q \quad (19)
 \end{aligned}$$

$$\begin{aligned}
 k_{bxy} &= \int_0^1 \int_0^1 \left( \frac{\partial^2 h}{\partial R \partial Q} \right)^2 dR dQ = \int_0^1 \left( \frac{\partial h_x}{\partial R} \right)^2 \partial R * \int_0^1 \left( \frac{\partial h_y}{\partial Q} \right)^2 \partial Q \\
 k_{bxy} &= \int_0^1 (1 - 6R^2 + 4R^3)^2 \partial R * \int_0^1 \left( \frac{7}{3} - 10Q^2 + \frac{40}{3}Q^3 - 5Q^4 \right)^2 \partial Q \\
 k_{bxy} &= \int_0^1 (1 - 12R^2 + 8R^3 + 36R^4 - 48R^5 + 16R^6) \partial R * \int_0^1 \left( \frac{49}{9} - \frac{140}{3}Q^2 + \frac{560}{9}Q^3 + \frac{230}{3}Q^4 \right. \\
 &\quad \left. - \frac{800}{3}Q^5 + \frac{2500}{9}Q^6 - \frac{400}{3}Q^7 + 25Q^8 \right) \partial Q \quad (20)
 \end{aligned}$$

$$\begin{aligned}
 k_{by} &= \int_0^1 \int_0^1 \left(\frac{\partial^2 h}{\partial Q^2}\right)^2 dRdQ = \int_0^1 h_x^2 \partial R * \int_0^1 \left(\frac{\partial^2 h_y}{\partial Q^2}\right)^2 \partial Q \\
 k_{by} &= \int_0^1 (R - 2R^3 + R^4)^2 \partial R * \int_0^1 (-20Q + 40Q^2 - 20Q^3)^2 \partial Q \\
 k_{by} &= \int_0^1 (R^2 - 4R^4 + 2R^5 + 4R^6 - 4R^7 + R^8) \partial R \\
 &\quad * \int_0^1 (400Q^2 - 1600Q^3 + 2400Q^4 - 1600Q^5 \\
 &\quad + 400Q^5) \partial Q \tag{21}
 \end{aligned}$$

$$\begin{aligned}
 k_{mx} &= \int_0^1 \int_0^1 \left(\frac{\partial h}{\partial R}\right)^4 dRdQ = \int_0^1 \left(\frac{\partial h_x}{\partial R}\right)^4 \partial R * \int_0^1 h_y^4 \partial Q \\
 k_{mx} &= \int_0^1 (1 - 6R^2 + 4R^3)^4 \partial R * \int_0^1 \left(\frac{7}{3}Q - \frac{10}{3}Q^3 + \frac{10}{3}Q^4 - Q^5\right)^4 \partial Q \\
 k_{mx} &= \int_0^1 (1 - 24R^2 + 16R^3 + 216R^4 - 288R^5 - 768R^6 + 1728R^7 + 144R^8 - 3200R^9 + 3456R^{10} \\
 &\quad - 1536R^{11} + 256R^{12}) \partial R * \int_0^1 \left(\frac{2401}{81}Q^4 - \frac{13720}{81}Q^6 + \frac{13720}{81}Q^7 + \frac{25284}{81}Q^8 \right. \\
 &\quad - \frac{58800}{81}Q^9 + \frac{19040}{81}Q^{10} + \frac{66360}{81}Q^{11} - \frac{96554}{81}Q^{12} + \frac{38400}{81}Q^{13} + \frac{39240}{81}Q^{14} \\
 &\quad - \frac{68440}{81}Q^{15} + \frac{50644}{81}Q^{16} - \frac{7600}{27}Q^{17} + \frac{720}{9}Q^{18} - \frac{40}{3}Q^{19} \\
 &\quad \left. + Q^{20}\right) \partial Q \tag{22}
 \end{aligned}$$

$$\begin{aligned}
 k_{mxy} &= \int_0^1 \int_0^1 \left(\frac{\partial h}{\partial R}\right)^2 \left(\frac{\partial h}{\partial Q}\right)^2 dRdQ = \int_0^1 \left(\frac{\partial h_x}{\partial R}\right)^2 . h_x^2 \partial R * \int_0^1 \left(\frac{\partial h_y}{\partial Q}\right)^2 . h_y^2 \partial Q \\
 k_{mxy} &= \int_0^1 (1 - 6R^2 + 4R^3)^2 * \left(\frac{7}{3}Q - \frac{10}{3}Q^3 + \frac{10}{3}Q^4 - Q^5\right)^2 \partial R \\
 &\quad * \int_0^1 (R - 2R^3 + R^4)^2 * \left(\frac{7}{3} - 10Q^2 + \frac{40}{3}Q^3 - 5Q^4\right)^2 \partial Q \\
 k_{mxy} &= \int_0^1 (R^2 - 16R^4 + 10R^5 + 88R^6 - 108R^7 - 159R^8 + 344R^9 - 60R^{10} - 296R^{11} + 292R^{12} \\
 &\quad - 112R^{13} + 16R^{14}) \partial R * \int_0^1 \left(\frac{2401}{81}Q^2 - \frac{27440}{81}Q^4 + \frac{34300}{81}Q^5 + \frac{95452}{81}Q^6 - \frac{264600}{81}Q^7 \right. \\
 &\quad + \frac{87780}{81}Q^8 + \frac{487340}{81}Q^9 - \frac{813714}{81}Q^{10} + \frac{355600}{81}Q^{11} + \frac{498520}{81}Q^{12} - \frac{958460}{81}Q^{13} \\
 &\quad + \frac{803260}{81}Q^{14} - \frac{136200}{27}Q^{15} + \frac{14500}{9}Q^{16} - \frac{900}{3}Q^{17} \\
 &\quad \left. + 25Q^{18}\right) \partial Q \tag{23}
 \end{aligned}$$

$$\begin{aligned}
 k_{my} &= \int_0^1 \int_0^1 \left(\frac{\partial h}{\partial Q}\right)^4 dRdQ = \int_0^1 h_x^4 \partial R * \int_0^1 \left(\frac{\partial^2 h_y}{\partial Q^2}\right)^4 \partial Q \\
 k_{my} &= \int_0^1 (R - 2R^3 + R^4)^4 \partial R * \int_0^1 \left(\frac{7}{3} - 10Q^2 + \frac{40}{3}Q^3 - 5Q^4\right)^4 \partial Q \\
 k_{my} &= \int_0^1 (R^4 - 8R^6 + 4R^7 + 24R^8 - 24R^9 - 26R^{10} + 48R^{11} - 8R^{12} - 28R^{13} + 24R^{14} - 8R^{15} \\
 &\quad + R^{16}) \partial R * \int_0^1 \left(\frac{2401}{81} - \frac{13720}{27}Q^2 + \frac{54880}{81}Q^3 + \frac{81340}{27}Q^4 - \frac{235200}{27}Q^5 - \frac{21000}{81}Q^6 \right. \\
 &\quad + \frac{890400}{27}Q^7 - \frac{1429950}{27}Q^8 + \frac{496000}{81}Q^9 + \frac{2559000}{27}Q^{10} - \frac{4468000}{27}Q^{11} \\
 &\quad + \frac{12320500}{81}Q^{12} - \frac{2360000}{27}Q^{13} + \frac{285000}{9}Q^{14} + \frac{20000}{3}Q^{15} \\
 &\quad \left. + 625Q^{16}\right) \partial Q \tag{24} \\
 k_{Nx} &= \int_0^1 \int_0^1 \left(\frac{\partial h}{\partial R}\right)^2 dRdQ = \int_0^1 \left(\frac{\partial h_x}{\partial R}\right)^2 \partial R * \int_0^1 h_y^2 \partial Q \\
 k_{Nx} &= \int_0^1 (1 - 6R^2 + 4R^3)^2 \partial R * \int_0^1 \left(\frac{7}{3}Q - \frac{10}{3}Q^3 + \frac{10}{3}Q^4 - Q^5\right)^2 \partial Q \\
 k_{Nx} &= \int_0^1 (1 - 12R^2 + 8R^3 + 36R^4 - 48R^5 + 16R^6) \partial R * \int_0^1 \left(\frac{49}{9}Q^2 - \frac{140}{9}Q^4 + \frac{140}{9}Q^5 + \frac{58}{9}Q^6 \right. \\
 &\quad \left. - \frac{200}{9}Q^7 + \frac{160}{9}Q^8 - \frac{20}{3}Q^9 + Q^{10}\right) \partial Q \tag{25}
 \end{aligned}$$

Integrating and substituting the values of R (= 0.5) and Q (= 1) at the point of maximum deflection, into Equations (19-24) yield the values of stiffness presented in roll 2 of Table 2 for the SSFS plate. Carrying out a similar evaluation for the remaining five boundary conditions yields the stiffness values presented in rolls 3 to 7 of Table 2.

Now substituting these values in Table 2, into Equation (5) and (6) yield equations for total bending and membrane stiffness expressions respectively as shown in Tables 3 and 4. And to obtain the specific postbuckling mathematical models for predicting the postbuckling load of a plate based on the boundary conditions under consideration, the total bending and membrane expression in Tables 2 and 3 were substituted into the general postbuckling equation in Equation (4) or (14). The postbuckling mathematical models are presented in Table 5.

**RESULTS AND DISCUSSIONS**

The results obtained from the preceding section are presented in this section. The numerical values of the individual stiffness of the six plates’ types under consideration are presented in Table 2.

Table 2: Stiffness Values for the Six Plate Edge Conditions

Plate Edge Condition	$k_{bx}$	$k_{bxy}$	$k_{by}$	$k_{mx}$	$k_{mxy}$	$k_{my}$	$k_{Nx}$
SSFS	4.0257816	1.0331066	0.1874528	0.3681508	0.0407665	0.0271358	0.4073708
SCFS	1.5096681	0.1823129	0.0287226	0.0127248	0.0013497	0.0007119	0.07188895
CSFS	0.3284779	0.0919002	0.1286676	0.0027493	0.0000921	0.0001995	0.0332388
CCFS	0.1231792	0.0162177	0.0197152	0.0000950	0.00000305	0.0000052	0.0058657
SCFC	0.6709636	0.04051398	0.0060469	0.0010902	0.00007699	0.0005114	0.0159753
CCFC	0.0547463	0.0036039	0.0041506	0.00000407	0.000000174	0.00000025	0.00130348

After substituting the values in Table 2 into Equations (5) and (6), we obtain the expression for total bending and membrane stiffness as presented in Tables 3 and 4 respectively.

Table 3: Total Bending Stiffness  $K_{bT}$  Equation for Six Plate Edge Condition

SSFS	$K_{bT} = \left[ 4.0257816258 + \frac{2.0662131519}{2^2} + \frac{0.1874527589}{2^4} \right]$
SCFS	$K_{bT} = \left[ 1.5096681097 + \frac{0.3646258503}{2^2} + \frac{0.0287226002}{2^4} \right]$
CSFS	$K_{bT} = \left[ 0.3284779221 + \frac{0.1838004535}{2^2} + \frac{0.1286675737}{2^4} \right]$
CCFS	$K_{bT} = \left[ 0.1231792208 + \frac{0.0324353741}{2^2} + \frac{0.0197151927}{2^4} \right]$
SCFC	$K_{bT} = \left[ 0.6709636043 + \frac{0.0810279667}{2^2} + \frac{0.0060468632}{2^4} \right]$
CCFC	$K_{bT} = \left[ 0.0547463203 + \frac{0.0072078609}{2^2} + \frac{0.0041505669}{2^4} \right]$

Table 4: Total Membrane Stiffness  $K_{mT}$  Equation for Six Plate Edge Conditions

Plate Condition	Edge	$K_{mT} = \left[ k_{mx} + \frac{2k_{mxy}}{2^2} + \frac{k_{my}}{2^4} \right]$
SSFS		$K_{mT} = \left[ 0.3681508201 + \frac{0.0815330290}{2^2} + \frac{0.0271358458}{2^4} \right]$
SCFS		$K_{mT} = \left[ 0.0127248132 + \frac{0.0026994824}{2^2} + \frac{0.0106024592}{2^4} \right]$
CSFS		$K_{mT} = \left[ 0.0027493343 + \frac{0.0001841873}{2^2} + \frac{0.0001994590}{2^4} \right]$
CCFS		$K_{mT} = \left[ 0.0000950284 + \frac{0.0000060983}{2^2} + \frac{0.0000052326}{2^4} \right]$
SCFC		$K_{mT} = \left[ 0.0010902116 + \frac{0.0001539812}{S^2} + \frac{0.0005114020}{S^4} \right]$
CCFC		$K_{mT} = \left[ 0.0000040708 + \frac{0.0000003479}{2^2} + \frac{0.0000002524}{2^4} \right]$

When the expressions in Tables 3 and 4 were substituted into Equation (4) or (14) which is the general postbuckling equation of thin plate we obtained the new formulated mathematical models for predicting the postbuckling load of thin plates as presented in Table 5.

Table 5: Buckling and Post buckling Load and Stress Equations for the Six Plate Edge Conditions

Plate Edge Condition	$N_x = \eta \frac{D}{a^2};$
SSFS	$N_x = \frac{1}{2^4} \left[ (9.88235294122^4 + 5.07207034982^2 + 0.4601527095) + (7.80817721872^4 + 1.72924873312^2 + 0.5755290525) \left( \frac{w}{t} \right)^2 \right] \frac{D}{a^2}$
SCFS	$N_x = \frac{1}{2^4} \left[ (212^4 + 5.07207034982^2 + 0.3995411967) + (9.55835131142^4 + 2.02773906782^2 + 7.9641271457) \left( \frac{w}{t} \right)^2 \right] \frac{D}{a^2}$
CSFS	$N_x = \frac{1}{2^4} \left[ (9.88235294122^4 + 5.52968960862^2 + 3.8710010320) + (7.94059344262^4 + 0.53196736812^2 + 0.5760749062) \left( \frac{w}{t} \right)^2 \right] \frac{D}{a^2}$
CCFS	$N_x = \frac{1}{2^4} \left[ (212^4 + 5.52968960862^2 + 3.3611111111) + (9.72044814302^4 + 0.62379170482^2 + 0.5352377090) \left( \frac{w}{t} \right)^2 \right] \frac{D}{a^2}$
SCFC	$N_x = \frac{1}{2^4} \left[ (422^4 + 5.07207034982^2 + 0.3785127127) + (14.74058997362^4 + 149.43877748502^2 + 6.9145910107) \left( \frac{w}{t} \right)^2 \right] \frac{D}{a^2}$
CCFC	$N_x = \frac{1}{2^4} \left[ (422^4 + 5.52968960862^2 + 3.1842105263) + (7.49528531482^4 + 0.64047062752^2 + 0.4647025071) \left( \frac{w}{t} \right)^2 \right] \frac{D}{a^2}$

To obtain the numerical value of the postbuckling load of each plate type considered here, the numerical values of  $w/t$  were substituted into the models in Table 5 to obtain the numerical values of postbuckling load coefficients of the plates as shown in Figure 1 and Table A1 for each plate type. While the stress parameter values are presented in Table A2 of the Appendix.

The above mathematical models have not been formulated before now. The new models are simple and easy to apply in predicting the buckling and postbuckling load of the plate types considered. The models can be used for any dimension of plates and can even be more compact when dealing with square plates, in which case the aspect ratio  $\lambda$  ( $=b/a$ ) is equal to unity. The models above can also predict separately the additional carrying capacity of a plate beyond its initial yield point. This will easily tell how much additional strength the plate has at a particular deformation. When the deformation,  $w$ , is zero, that is, when the plate is still flat and has not bent, the postbuckling load will be zero, in which case the postbuckling term in equation (14) will be zero given rise to the critical load of the plate. Figure 1 shows that the various plate considered have a gradual increase in strength beyond the initial yield. The situation that is a true behavior of plates unlike columns (Szilard 2004; Oguaghamba, 2015, O. Civalek, and A. Yavas, 2006; Katsikadelis, J. T. and Babouskos, N., 2007; Elsami, 2018). The chart shows that SCFC has the highest postbuckling strength while CSFS has less postbuckling strength for the six plate type with one free age.

To ascertain the validity of these models, the numerical results obtained from the mathematical models were compared with those in literature as shown in Table 6. Table 6 shows the comparison of the critical load obtained from these models with those of Ibearugbulem et al. (2014) who obtained theirs based on small deflection theory and also with those of Adah (2016). The results indicated a close agreement with those of Ibearugbulem et al. (2014) with a maximum percentage difference of 18.6% for SCFS while the remaining plate types' percentage differences are less the 15%. However, the results agreed with those of Adah earlier studies. It is worth noting that, there is a dearth of literature concerning the postbuckling strength of these boundary conditions of the plate due to the difficulties of analyzing plates under large deflection. One can infer that if the critical values predicted from these models are adequate and the postbuckling behaviors of the plates agreed with those in literature, then the postbuckling values predicted from these models are also considered adequate.

Buckling/Postbuckling Load Coeff. vs w/t

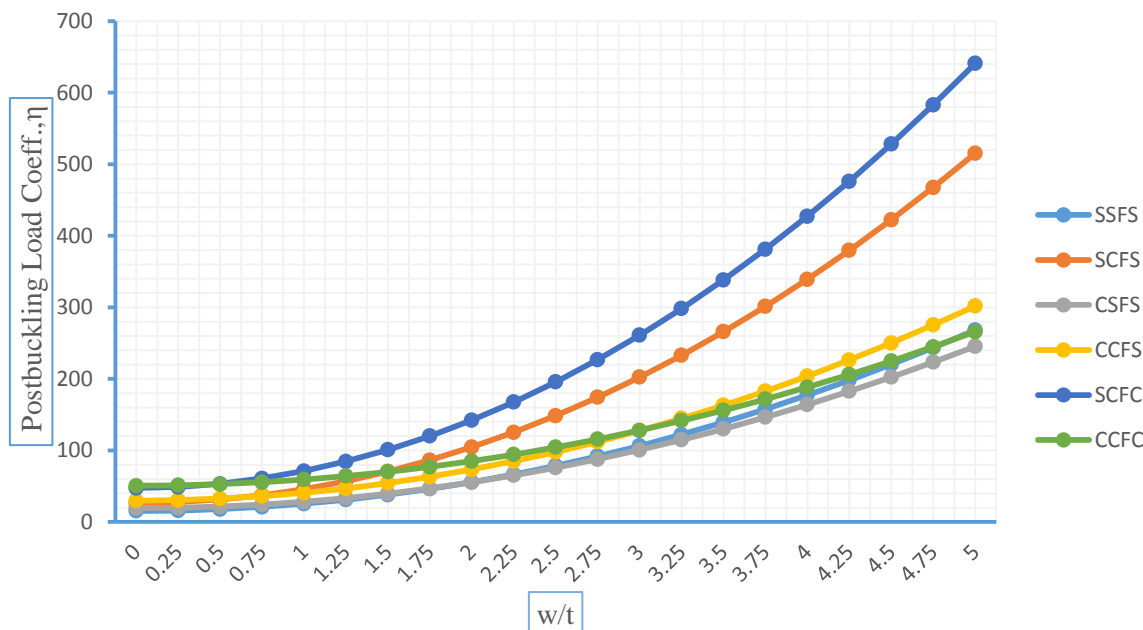


Table 6: Comparison of Critical Load of this Study with Earlier Studies.

BCs	SSFS	SCFS	CSFS	CCFS	SCFC	CCFC
Present ( $N_{cr}$ )	15.415	26.472	19.283	29.891	47.451	50.714
Ibearugbulem et al. (2014)	13.295	21.547	16.945	27.553	45.331	48.376
Adah, (2016)	15.415	26.472	19.283	29.891	47.451	50.714
%Diff 1	13.7528381	18.60456	12.12467	7.821752	4.467767	4.610167
%Diff 2	0	0	0	0	0	0

**CONCLUSION**

The present study has evaluated the shape profiles of six plates’ boundary conditions, that is, those with one free edge, to obtain the individual stiffness of each plate type. Based on these stiffnesses the specific postbuckling mathematical models for the plates considered were formulated. These models were used to predict the postbuckling behavior of thin plates under consideration. This is an attempt in providing simple models for analysts and designers of plated structures and to expand the volume of knowledge in the area of large deformation of plates. The adequacy of these models was tested with those in literature and was found adequate. Based on this, it was concluded that the present postbuckling mathematical models can be used to predict the postbuckling strength of these plates considered here and the approach can

easily be extended to other plates’ boundary conditions.

**REFERENCES**

Adah, E. I., 2016. "Development of Computer Programs for Analysis of Single Panel and Continuous Rectangular Plates" M. Eng. Thesis Federal University of Technology Owerri ([www.library.futo.edu.ng](http://www.library.futo.edu.ng)).

Adah, E. I., 2019. "Buckling and Postbuckling Analysis of SSSS Rectangular Plates using Modified Iyengar’s Equation" IOSR Journal of Mechanical and Civil Engineering, 16 (2), 35-40.

- Byklum, E. and Amdahl, J., 2002. "A simplified method for elastic large deflection analysis of plates and stiffened panels due to local buckling" *Thin-Walled Structures* 40 (11), 925–953.
- Civalek, O. and Yavas, A., 2006. "Large Deflection Static Analysis of Rectangular Plates on Two Parameters Elastic Foundations" *International Journal of Science and Technology*, 1(1), 43-50.
- Elsami, M. R., 2018. "Buckling and Postbuckling of Beams, Plates, and Shells" Springer International Publishing AG.
- Elsheikh, A. and Wang, D., 2005. "Large-Deflection Mathematical Analysis of Rectangular Plates", *Journal of Engineering Mechanics*, 131 (8).
- Enem, J. I., 2018. "Geometrically Nonlinear Analysis of Isotropic Rectangular Thin Plates Using Ritz Method" PhD Thesis Federal University of Technology, Owerri Nigeria ([www.library.futo.edu.ng](http://www.library.futo.edu.ng)).
- Eziefula, U. G., Ibearugbulem, O. M. and Onwuka, D. O., 2014. "Plastic Buckling Analysis of an Isotropic C-SS-SS-SS Plate under in-plane Loading using Taylor's Series Displacement Function" *International Journal of Engineering and Technology*, 4(1), 17-22.
- GhannadPour, S. A. M. and Alinia, M. M., 2006. "Large deflection behavior of functionally graded plates under pressure loads", *Composite Structures*, 75, 67–71.
- Ibearugbulem, O. M., Onwuka, D. O. and Eziefula, 2013. "Inelastic Buckling Analysis of Axially Compressed Thin CCCC Plates using Taylor-Maclaurin Displacement Function" *Academic Research International Part III: Natural & Applied Sciences*, 4(6), 594-600.
- Ibearugbulem, O. M., Ezech, J. C. and Ettu, L. O., 2014. *Energy Methods in Theory of Rectangular Plates: Use of Polynomial Shape Functions*. Owerri, Liu House of Excellence Ventures.
- Ibearugbulem, O. M., Adah, E. I., Onwuka, D. O. and Okere, C. E., 2020. Simple and Exact Approach to Postbuckling Analysis of Rectangular Plate, SSRG *International Journal of Civil Engineering*, 7 (6): 54-64, [www.internationaljournalsrsg.org](http://www.internationaljournalsrsg.org).
- Katsikadelis, J. T. and Babouskos, N., 2007. "The Postbuckling Analysis of Plates: A BEM Based Meshless Variational Solution" *Mechanical Automatic Control and Robotics*, 6(1), 113-118.
- Muraddova, A. D. and Stavroulakis, G. S., 2012. "Buckling and Postbuckling Analysis of Rectangular Plates Resting on Elastic Foundations with the use of the Spectral Method" *Comput. Methods Appl. Mech. Engrg.* 213-220.
- Oguaghamba, O. A., 2015. "Analysis of buckling and postbuckling loads of Isotropic thin rectangular plates" PhD Thesis Federal University of Technology, Owerri Nigeria ([www.library.futo.edu.ng](http://www.library.futo.edu.ng)).
- Onodagu, P. D., 2018. "Nonlinear Dynamic Analysis of Thin Rectangular Plates using Ritz Method" PhD Thesis Federal University of Technology, Owerri Nigeria ([www.library.futo.edu.ng](http://www.library.futo.edu.ng)).
- Paik, J. K, Park, J. H. and Kim, B. J., 2012. Analysis of Elastic Large Deflection for Metal Plates under Non-uniformly Distributed Lateral of Pressure with In-plane Loads. *Journal of Applied Mathematics*.
- Shufrin, I., Rabinovitch, O. and Eisenberger, M., 2008. "A semi-analytical approach for the nonlinear large deflection analysis of laminated rectangular plates under general out-of-plane loading" *International Journal of Non-Linear Mechanics*, 43, 328–340.
- Szillard, R., 2004. *Theories and Application of Plate Analysis*, John Wiley & Sons, New Jersey.
- Tanriöver, H. and Senocak, E., 2004. "Large deflection analysis of unsymmetrically laminated composite plates: analytical-numerical type approach", *International Journal of Non-linear Mechanics*. 39, 1385–1392.
- Yoo, C. H., and Lee, S. C., 2011. *Stability of Structures: Principles and Applications*. Butterworth-Heinemann, UK.

APPENDICES

Table A1: Numerical Values of Buckling and Postbuckling Coefficient,  $\eta$ , of Rectangular plates for the Six Plates with one Free Edge.

$N_x = \eta \frac{D}{a^2}; \quad z = \frac{b}{a} = 1$						
$\eta = \left[ \frac{K_{bT}}{k_{Nx}} + \frac{3 K_{mT}}{2 k_{Nx}} \frac{1}{(h_{\max})^2} \left( \frac{w}{t} \right)^2 \right]$						
w/t	SSFS	SCFS	CSFS	CCFS	SCFC	CCFC
0	15.415	26.472	19.283	29.891	47.451	50.714
0.25	16.047	27.694	19.849	30.571	48.934	51.251
0.5	17.943	31.359	21.545	32.611	53.385	52.864
0.75	21.103	37.469	24.373	36.011	60.803	55.552
1	25.528	46.022	28.332	40.770	71.188	59.314
1.25	31.216	57.019	33.422	46.890	84.540	64.152
1.5	38.169	70.460	39.642	54.370	100.859	70.065
1.75	46.386	86.344	46.994	63.209	120.146	77.053
2	55.866	104.672	55.478	73.409	142.399	85.116
2.25	66.611	125.445	65.092	84.968	167.620	94.254
2.5	78.621	148.660	75.837	97.888	195.808	104.467
2.75	91.894	174.320	87.713	112.167	226.963	115.755
3	106.431	202.424	100.721	127.806	261.085	128.118
3.25	122.233	232.971	114.859	144.805	298.174	141.556
3.5	139.298	265.962	130.129	163.164	338.231	156.070
3.75	157.628	301.397	146.529	182.883	381.254	171.658
4	177.222	339.275	164.061	203.962	427.245	188.321
4.25	198.080	379.597	182.724	226.401	476.203	206.060
4.5	220.202	422.364	202.518	250.200	528.128	224.873
4.75	243.588	467.573	223.443	275.359	583.020	244.762
5	268.238	515.227	245.499	301.878	640.879	265.725

Table A2: Numerical Values of Stress Parameter  $\frac{\sigma_x a^2}{Et^2}$  for Six Plate Edge Conditions

$$\frac{\sigma_x a^2}{Et^2} = \frac{1}{12(1-\nu^2)k_{Nx}} \left[ K_{bT} + \frac{3}{2} \frac{1}{(h_{\max})^2} \left(\frac{w}{t}\right)^2 K_{mT} \right]; \nu = 1$$

w/t	SSFS	SCFS	CSFS	CCFS	SCFC	CCFC
0	1.412	2.424	1.766	2.737	4.345	4.644
0.25	1.469	2.536	1.818	2.800	4.481	4.693
0.5	1.643	2.872	1.973	2.986	4.889	4.841
0.75	1.933	3.431	2.232	3.298	5.568	5.087
1	2.338	4.214	2.594	3.734	6.519	5.432
1.25	2.859	5.222	3.061	4.294	7.742	5.875
1.5	3.495	6.452	3.630	4.979	9.236	6.416
1.75	4.248	7.907	4.304	5.788	11.002	7.056
2	5.116	9.585	5.080	6.722	13.040	7.794
2.25	6.100	11.488	5.961	7.781	15.350	8.631
2.5	7.200	13.614	6.945	8.964	17.931	9.567
2.75	8.415	15.963	8.032	10.272	20.784	10.600
3	9.746	18.537	9.224	11.704	23.909	11.732
3.25	11.193	21.334	10.518	13.261	27.305	12.963
3.5	12.756	24.355	11.917	14.942	30.973	14.292
3.75	14.435	27.600	13.418	16.748	34.913	15.720
4	16.229	31.069	15.024	18.678	39.125	17.246
4.25	18.139	34.762	16.733	20.733	43.608	18.870
4.5	20.165	38.678	18.546	22.912	48.363	20.593
4.75	22.307	42.818	20.462	25.216	53.390	22.414
5	24.564	47.182	22.482	27.644	58.689	24.334